Zhou et al. Nanoscale Research Letters (2017) 12:354
DOI 10.1186/s11671-017-2115-8

Nanoscale Research Letters

NANO EXPRESS Open Access

Surface Morphology Evolution Mechanisms of InGaN/GaN Multiple Quantum Wells with Mixture N_2/H_2-Grown GaN Barrier

Xiaorun Zhou[1,2], Taiping Lu[1,2*], Yadan Zhu[1,2], Guangzhou Zhao[1,2], Hailiang Dong[1], Zhigang Jia[1,2], Yongzhen Yang[1,2*], Yongkang Chen[1] and Bingshe Xu[1,2]

Abstract

Surface morphology evolution mechanisms of InGaN/GaN multiple quantum wells (MQWs) during GaN barrier growth with different hydrogen (H_2) percentages have been systematically studied. Ga surface-diffusion rate, stress relaxation, and H_2 etching effect are found to be the main affecting factors of the surface evolution. As the percentage of H_2 increases from 0 to 6.25%, Ga surface-diffusion rate and the etch effect are gradually enhanced, which is beneficial to obtaining a smooth surface with low pits density. As the H_2 proportion further increases, stress relaxation and H_2 over-etching effect begin to be the dominant factors, which degrade surface quality. Furthermore, the effects of surface evolution on the interface and optical properties of InGaN/GaN MQWs are also profoundly discussed. The comprehensive study on the surface evolution mechanisms herein provides both technical and theoretical support for the fabrication of high-quality InGaN/GaN heterostructures.

Keywords: GaN barrier, Hydrogen, Surface, Interface

Background

InGaN/GaN-based high-brightness light-emitting diodes (LEDs) and laser diodes, as the representative devices of III-nitrides, have attracted much attention owing to their important role in digital signage, high-density optical storage, and general illumination [1–10]. Generally speaking, fabrication of blue or green LEDs requires relatively high indium composition of InGaN layer [11, 12]. Although the reduction of growth temperature and the increase of growth rate of the quantum well (QW) can alleviate indium atom desorption to obtain high indium content, these methods also deteriorate the optical performance of InGaN/GaN multiple quantum wells (MQWs) by worsening interface abruptness and introducing more defects [13, 14]. Moreover, these defects usually act as nonradiative recombination centers, thus weakening the internal quantum efficiency of the device [15–19]. Therefore, achieving required indium content while maintaining high material quality is still a big challenge.

In order to settle the problems mentioned above, various growth techniques have been employed in striving for smooth morphology and sharp interfaces within the InGaN/GaN stack. Quantum barriers (QBs) grown at elevated temperature [20, 21] and growth interruption after QWs [12, 22] are widely used to improve the morphology of InGaN/GaN heterostructures. However, they all have their own limitations. For instance, barriers grown at high temperature may lead to severe In loss [14, 23]. Although growth interruption can improve morphology as well as reduce inclusions, it is at the expense of the optical quality of the QWs [21]. Recently, it is reported that introducing a small amount of hydrogen during the growth of GaN barriers can improve both optical and interface properties [24–28]. However, the effect mechanism of H_2 on surface evolution of InGaN/GaN MQWs has not been fully understood yet.

In this paper, the effects of H_2 proportion, defined as H_2 flow divided by total carrier gas flow, during GaN barrier deposition, on surface morphology evolution are systematically investigated. Ga surface-diffusion rate,

* Correspondence: lutaiping@tyut.edu.cn; yyztyut@126.com
[1]Key Laboratory of Interface Science and Engineering in Advanced Materials, Ministry of Education, Taiyuan University of Technology, Taiyuan 030024, China
Full list of author information is available at the end of the article

Springer Open

© The Author(s). 2017 **Open Access** This article is distributed under the terms of the Creative Commons Attribution 4.0 International License (http://creativecommons.org/licenses/by/4.0/), which permits unrestricted use, distribution, and reproduction in any medium, provided you give appropriate credit to the original author(s) and the source, provide a link to the Creative Commons license, and indicate if changes were made.

stress relaxation, and H_2 etching effect are suggested to be the three main factors, affecting surface evolution. The dominant factors and their influences on the surface evolution are comprehensively discussed, which provides a technical guideline to obtain high-quality InGaN/GaN heterostructures.

Methods

The InGaN/GaN MQW structures were grown on c-plane sapphire substrate by Aixtron TS300 metal organic chemical vapor deposition system. Trimethylgallium (TMG), triethylgallium (TEG), trimethylindium (TMI), and ammonia (NH_3) were used as precursors. Silane (SiH_4) was used as the n-type dopant source. The structure was composed of 3.2-μm-thick undoped GaN layer and nominally six-period 2.4-nm-thick InGaN QWs separated by 11-nm-thick lightly Si-doped (n-doping = $3\times10^{17}cm^{-3}$) GaN barriers. A 1.0-nm-thick low temperature GaN cap layer (LT-GaN) was deposited immediately after the growth of QW layer. InGaN wells and GaN barriers were grown at 730 and 850 °C, respectively. A conventional InGaN/GaN MQWs sample, labeled as S_1, was grown in nitrogen atmosphere. Four other samples, denoted as S_2, S_3, S_4, and S_5, were grown with different proportion of H_2 flow to total carrier gas ($N_2 + H_2$) during barriers deposition, with the other growth parameters the same with S_1. The percentage of H_2 was 2.5% (S_2), 6.25% (S_3), 10% (S_4), and 50% (S_5), respectively.

The structures of InGaN/GaN MQWs were characterized by PANalytical Empyrean high resolution x-ray diffraction (HRXRD) system. Surface morphology was obtained by atomic force microscopy (AFM) (SPA-300HV) using tapping model. Room temperature (RT) photoluminescence (PL) properties of the samples were studied by 226-nm Nd-YAG laser with an excitation power density of 1.36 W/cm^2.

Results and Discussion

The HRXRD ω-2θ scanning results of S_1–S_5 are illustrated in Fig. 1a. The strongest peak located at the center belongs to the underlying GaN template, and the satellite peaks correspond to the periodicity of the MQWs. It is found that the full-width at half-maximum (FWHM) of the strongest peaks in all samples is almost the same, indicating the similar crystal quality of GaN buffer layers for all samples. The presence of clearly distinguished "+4th" diffraction peak in samples S_2–S_4 manifest the improvement of crystal quality under low H_2 percentage. The appearance of the "+5th" diffraction peak (represented by the rectangle in Fig. 1a) and the minimum FWHM value of InGaN "−1st" diffraction peak indicate the best interface quality in sample S_3. The structure parameters determined by fitting the measured XRD curves are summarized in Table 1. The period thicknesses of the five samples are almost the same, and the values keep around 14.4 nm. The indium contents of the InGaN wells for samples S_1 to S_4 keep around 11.8%, while the value drops to 9.9% for S_5. A large amount of H_2 may etch the GaN LT-cap layer and then react with indium atoms in QWs, which result in the reduction of average indium content [29]. The roughness of the interface can be calculated by fitting FWHM of the XRD satellite peak by the following equation [26, 30]:

$$\Delta\omega_n = \Delta\omega_0 + \left[(\ln 2)^{1/2}\cdot \Delta\theta_M \cdot \frac{\gamma}{D}\right]\cdot n \quad (1)$$

where $\Delta\omega_n$ represents the FWHM of the n-th satellite peak, $\Delta\omega_0$ is the intrinsic width of satellite peaks, $\Delta\theta_M$ is the angle spacing between the adjacent satellite peaks, D is the period thickness of the InGaN/GaN MQW and γ is the interface roughness. Figure 1b shows the linear relationship between FWHMs and satellite peak orders. The slope of the fitting line is related to the QW/QB interface roughness. The fitting results show that

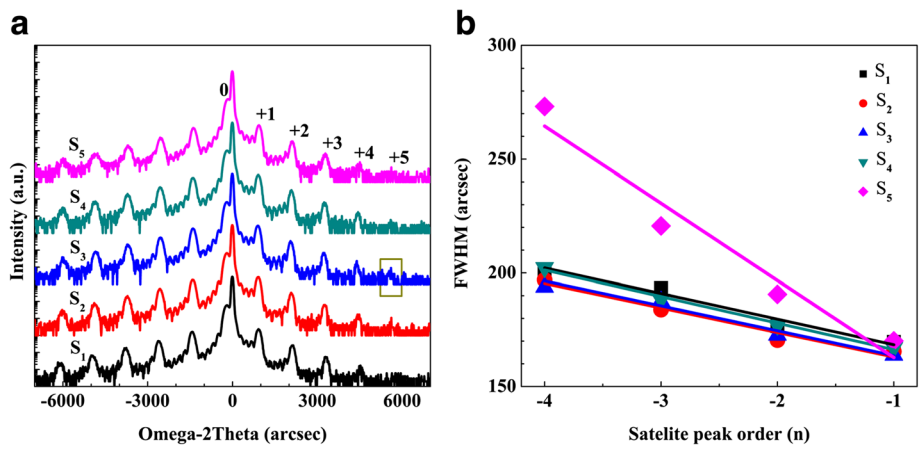

Fig. 1 **a** The HRXRD ω-2θ scanning results of S_1–S_5. **b** The FWHM as a function of the satellite peak order and its linear fitting for the five samples

Table 1 Structure parameters of InGaN/GaN MQWs determined by HRXRD fitting

Sample	H_2 percentage (%)	In content (%)	FWHM of InGaN "−1st" diffraction peak (arcsec)	Slope of liner fitting
S_1	0	11.84	169.66	−11.27
S_2	2.50	12.04	165.43	−10.79
S_3	6.25	11.67	163.77	−10.49
S_4	10	11.60	167.19	−11.68
S_5	50	9.90	170.13	−33.92

interface roughness is gradually reduced as the H_2 percentage increases, and the optimum value is achieved at 6.25% of H_2 (S_3), as shown in Table 1. With further raising in the percentage to 50% (S_5), the interface roughness is increased dramatically. Hence, the ratio of H_2 during barrier growth has great impact on interface quality. A small percentage (0–6.25%) of H_2 is favorable to obtaining sharp interface, while a large amount of H_2 (50%) seriously roughens the interface.

The AFM images of sample S_1–S_5 are shown in Fig. 2a–e. The dark points are mainly V-pits [14, 31], which initiate at the threading dislocations (TDs) [21, 27]. The root mean square (RMS) surface roughness under different H_2 percentage is illustrated in Fig. 3. The reference sample S_1 grown with H_2-free condition possesses the coarsest surface with an RMS roughness of 1.028 nm. The RMS value decreases with the increase of H_2 percentage, and achieves the minimum value (0.705 nm) at 6.25% of H_2, as shown in Fig. 3. As the H_2 percentage raises to 10%, the surface gets slightly rougher. With further increase in H_2 percentage to 50%, many large holes are formed, as pointed out by red arrows in Fig. 2, and surface RMS roughness dramatically increases to 0.924 nm.

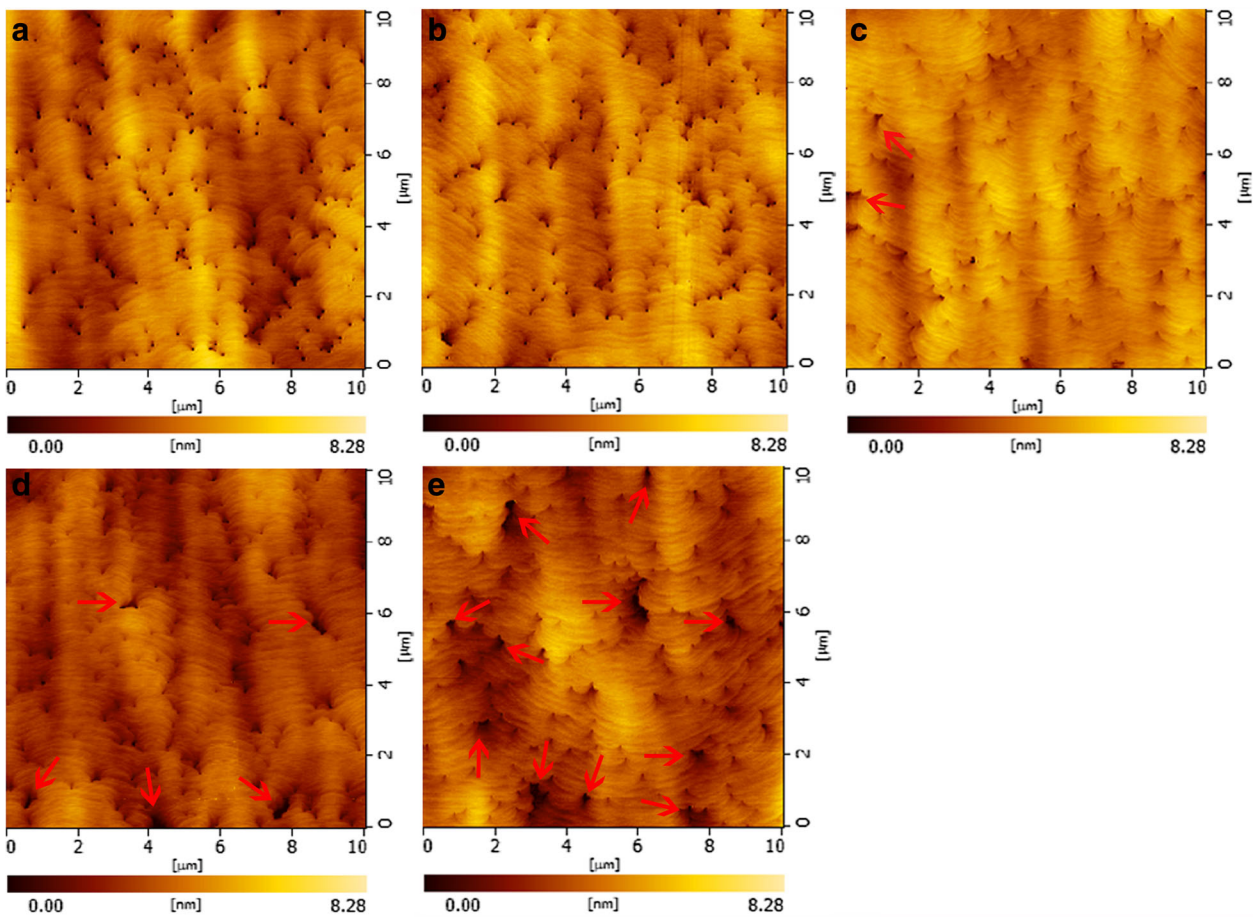

Fig. 2 The AFM images (10 × 10 μm) of five samples: **a** S_1, **b** S_2, **c** S_3, **d** S_4, and **e** S_5

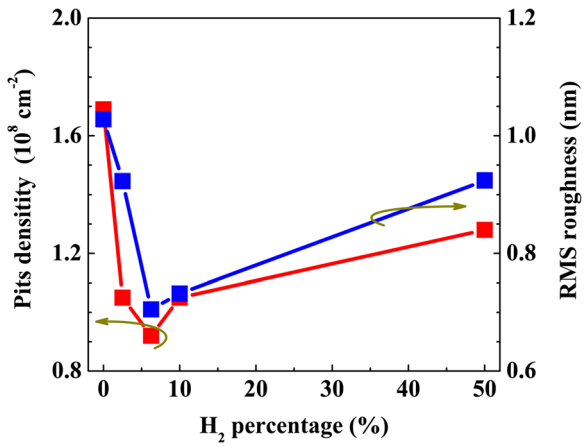

Fig. 3 The variation trend of pits density and RMS surface roughness under different H_2 percentage in carrier gas during the growth of barriers

Figure 4 shows the statistical calculated diagram of pits size distributions for the five samples. It can be seen that as 2.5% H_2 is introduced, the smallest pits (<60 nm) start to emerge, and the largest pits (>160 nm) disappear. As H_2 percentage increases to 6.25% (S_3), the proportion of pits at size 80–100 nm is significantly raised, and that of large pits (>140 nm) is dramatically reduced to the minimum value. With further increase in the H_2 percentage to 10%, the largest pits begin to emerge again. When 50% H_2 is introduced, the ratio of large pits is dramatically increased. Hence, the pits size can be reduced by introducing a small amount of H_2, and the optimum value is acquired at 6.25% percentage. However, the pits size shows an increase trend as H_2 percentage further rises.

It is obvious that the evolution trend of RMS surface roughness is highly consistent with that of pits size, which may relate to the growth mode affected by the formed pits. Once the pits are formed, indium atoms will first nucleate at the point where the TDs intersect the InGaN/GaN interface [32–35], then island growth starts and finally island growth mode transfers to 2-Dimensional growth. In other words, the presence of V-pits will delay the 2-dimensional growth, then roughen the surface. The larger the size is, the more obvious the delay can be.

In order to elucidate the surface evolution mechanism under different H_2 percentages, the variation trend of V-pits size is discussed in detail. As H_2 percentage increases from 0 to 6.25%, the decrease in V-pits size possibly comes from the following two parts. First, the formed Ga-H complex may enhance the incorporation efficiency of Ga atoms on $\{10\bar{1}1\}$ plane [35]. It is reported that the adsorption energy of the Ga-H complex is about 1.2 eV smaller than that of single Ga adatoms [28]. Hence, the attachment of hydrogen to Ga adatom could significantly

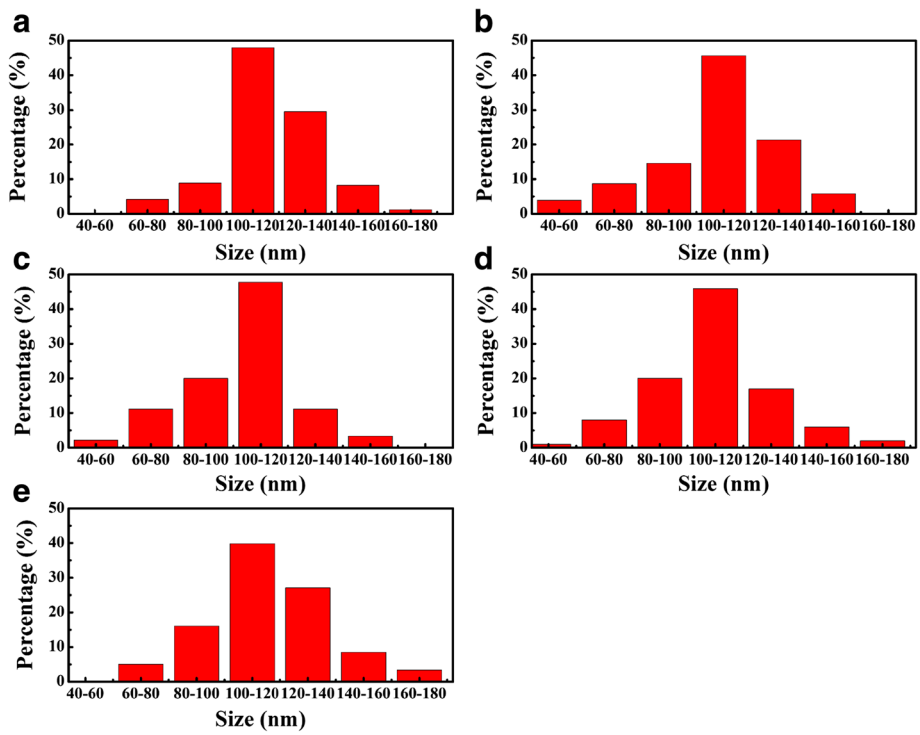

Fig. 4 The distribution of pit size for the five samples: **a** S_1, **b** S_2, **c** S_3, **d** S_4, and **e** S_5

weaken the bond to the surface, which benefits the surface diffusion of Ga atoms [28, 36]. Another important reason is the gradually enhanced etching effect with the increase of H_2 percentage. Shiojiri et al. reported that indium atoms can be easily trapped and segregated around the core of TDs, which plays a role of a small mask that hinders Ga atoms migration [37]. Hence, introducing H_2 during the growth can effectively eliminate indium-rich clusters at InGaN/GaN interface, and contribute to surface migration of Ga atoms [37–39]. In addition, hydrogen can etch some unstable areas, such as dislocation sites and V-pits [40–43]. It is reported that dislocation sites are unstable due to the high strain energy and weak binding energy, and these sites can be easily dissociated during the etching process [41–43]. Moreover, the V-pit commonly consists of six symmetric N-terminated $\{10\bar{1}1\}$ facets [44, 45], which is much weaker during the etching process as compared with Ga-terminated facets [42, 43]. Therefore, when H_2 arrives at the surface, it is difficult to etch most of the GaN on the surface due to the high stability of Ga-face. Thus, H_2 etching occurs mainly at dislocation sites and V-pits [42, 43], causing the decomposition of GaN. Due to the low growth temperature of GaN barrier, the decomposition effect of GaN is weak when hydrogen percentage is low [26]. Hence, the enhanced Ga atoms incorporation plays a dominate role in surface evolution, which is beneficial in reducing the size and density of pits and in turn enhances the 2-Dimensional growth and suppresses the formation of new pits, and finally conductive to smooth surface. The correlation between pits density and H_2 percentage is presented in Fig. 3. It is shown that the highest pit density (1.69×10^8 cm^{-2}) exists in the H_2-free sample. While a small amount of H_2 is added in the carrier gas, pits density is gradually reduced and reaches the lowest value (0.92×10^8 cm^{-2}) in sample S_3. With further increase in H_2 proportion to 50%, pits density is significantly increased to 1.28×10^8 cm^{-2}. These results indicate that adding a little H_2 in the growth of barrier layer can suppress the formation of new pits. However, the suppression of new pits formation could lead to strain accumulation inside the layer, and the strain may relax via formation of new dislocations and other defects such as big pits in S_4 and S_5 [21], which will deteriorate the quality of the surface, as well as the InGaN/GaN interface.

It is worth to mention that the large holes (>200 nm) as marked with red arrows do not appear in samples S_1 and S_2, and they only start to appear as H_2 percentage becomes larger than 2.5%. The hole size in S_5 is much larger than that in samples S_3 and S_4, which may relate to the following two possible mechanisms about hydrogen over-etching mechanisms. One is the hydrogen over-etching on dislocation sites and V-pits. As aforementioned, the enhanced diffusion of Ga atoms plays a dominant role when hydrogen percentage is low. However, this leading role shifts to the enhanced GaN decomposition around dislocation sites and V-pits when large amounts of hydrogen are applied. The hydrogen can diffuse along the dislocation line and then etch the surrounded unstable sites both vertically and longitudinally, which could decrease the average indium contents in MQWs region, degrade well/barrier interface quality and also form large holes on the surface. Another possible mechanism is about hydrogen over-etching on LT-GaN cap layer. As H_2 proportion lower than 2.5%, the H_2 etch effect on LT-GaN cap layer is negligible. As the H_2 percentage increases to 10%, the H_2 etch effect on LT-GaN cap is illustrated in Fig. 5a. H_2 only etches a part of the cap layer, which has little influence on the QW layer, as evidenced by almost unchanged indium contents, and positive influence on the surface morphology, as confirmed by low pits density and small size of the holes. However, under large H_2 percentage, the LT-GaN cap layer may be partly etched away and QW layer be directly exposed to H_2, as presented in Fig. 5b. Under this case, H_2 will react with indium atoms in QW layer, leading to significant indium loss, large size, and high-density holes, and consequently dramatically deteriorates InGaN/GaN interface and surface qualities. Hence, surface morphology evolution is an integrated effect of surface diffusion rate, strain relaxation and H_2 etch effect. For sample S_2 and S_3 with H_2 percentage lower than 6.25%, gradually enhanced surface diffusion rate and H_2 etch effect play a dominant role, which contributes to smoother surface and lower pits density. With further

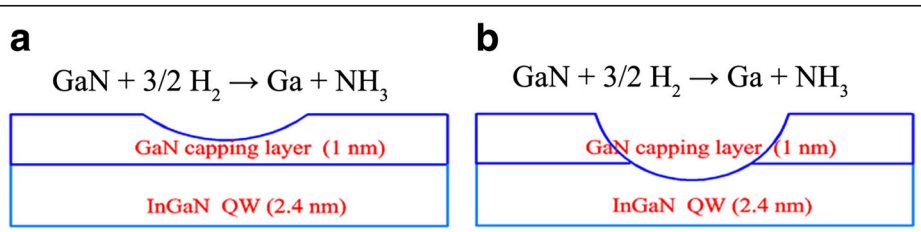

Fig. 5 **a** The etch effect on LT-GaN cap layer with H_2 percentage lower than 10%. **b** the H_2 over etch effect on LT-GaN capping layer under large H_2 percentage

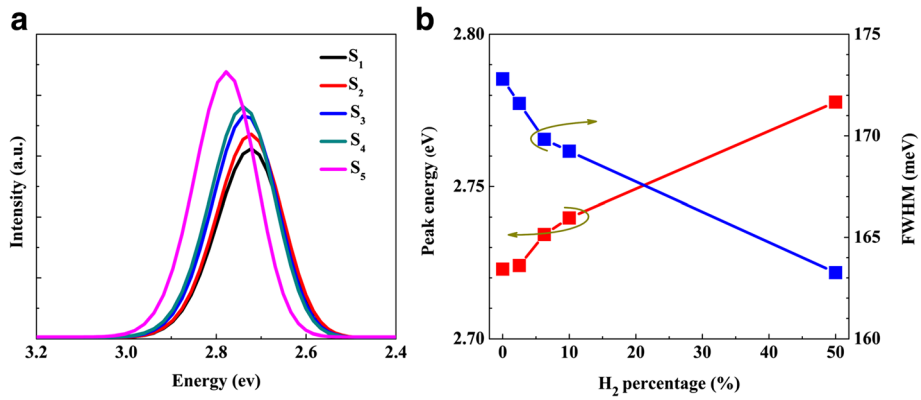

Fig. 6 a The measured room temperature PL spectra of the samples. **b** Gaussian-fitted FWHM and peak energy versus H_2 percentage in carrier gas

increase in the percentage to 10% (S_4), surface properties become slightly worse as a result of stress relaxation. The surface morphology of sample S_5 grown in 50% H_2 is mainly controlled by H_2 over-etching effect and strain relaxation in InGaN QWs, which leads to many large holes and the worst surface.

Figure 6a shows the measured room temperature PL spectra of the five samples. It can be seen that the PL intensity shows an increase trend and peak energy exhibits blue-shift as H_2 percentage increases. Compared with that of sample S_1 without H_2, the integrated PL intensity of samples S_2–S_5 is increased by 7.0, 15.8, 19.3, and 31.6%, respectively. For samples S_2–S_4, slightly blue-shifted peak energy and reduced FWHM are observed, as shown in Fig. 6b. As aforementioned, the structure parameters of sample S_2–S_4 are quite similar. Hence, the slightly changed spectral characteristics along with enhanced PL intensity are mainly caused by the enhanced surface and interface quality, and the partial relaxation of stress in QWs alleviating quantum confined stark effect (QCSE) [21, 46]. In contrast, the significantly reduced FWHM, blue-shifted peak energy and enhanced PL intensity of sample S_5 may result from strain relaxation and the lowest indium content caused by H_2 over-etching effect, both of which can greatly alleviate QCSE effect in MQWs [46–49]. In addition, H_2 can eliminate impurities such as carbon and oxygen in active region, which would benefit the improvement of the PL intensity [50, 51].

Conclusions

In summary, the effect of H_2 percentage during the barriers growth on InGaN/GaN MQWs properties has been systematically studied. As a small percentage of H_2 (≤6.25%) is introduced, the combined effect of enhanced H_2 etch effect and surface diffusion contribute to the improvement of surface, interface and optical properties. In spite of the strongest PL intensity achieved by introducing large percentage H_2 (50%), the integrated effect of H_2 over-etching and stress relaxation degrades surface and interface quality of the InGaN/GaN MQWs. Hence, the use of H_2 with appropriate proportion during the barriers growth can achieve smooth surface with low pits density and enhanced optical performance. The profound discussions of surface evolution mechanism here clearly depict the physical pictures of surface evolution process under different growth conditions, which is helpful for the fabrication of high-quality GaN-based devices.

Abbreviations

AFM: Atomic force microscopy; HRXRD: High-resolution x-ray diffraction; LED: Light-emitting diode; RMS: Root mean square; PL: Photoluminescence

Acknowledgements

This work was supported by National Natural Science Foundation of China (Grant Nos. 61504090, 21471111 and 61604104), the Applied Basic Research Projects of Shanxi Province (Grant No. 2016021028), the National Key R&D Program of China (2016YFB0401803), and the Shanxi Provincial Key Innovative Research Team in Science and Technology (Grant No. 201605D131045-10).

Authors' contributions

XZ and TL conceived the study. XZ, YZ, and GZ conducted the sample-growth and test experiments. TL supervised the entire research project. XZ, TL, YZ, GZ, HD, ZJ, YY, YC, and BX analyzed the data. All authors discussed the results and wrote the manuscript. All authors read and approved the final manuscript.

Competing interests

The authors declare that they have no competing interests.

Publisher's Note

Springer Nature remains neutral with regard to jurisdictional claims in published maps and institutional affiliations.

Author details

[1]Key Laboratory of Interface Science and Engineering in Advanced Materials, Ministry of Education, Taiyuan University of Technology, Taiyuan 030024, China. [2]Research Center of Advanced Materials Science and Technology, Taiyuan University of Technology, Taiyuan 030024, China.

Received: 12 March 2017 Accepted: 27 April 2017
Published online: 16 May 2017

References

1. Zhang Z-H, Liu W, Ju Z, Tiam Tan S, Ji Y, Kyaw Z et al (2014) Self-screening of the quantum confined Stark effect by the polarization induced bulk charges in the quantum barriers. Appl Phys Lett 104(24):243501
2. Liu G, Zhao H, Zhang J, Park JH, Mawst LJ, Tansu N (2011) Selective area epitaxy of ultra-high density InGaN quantum dots by diblock copolymer lithography. Nanoscale Res Lett 6(1):342
3. Zhang J, Tansu N (2013) Optical gain and laser characteristics of InGaN quantum wells on ternary InGaN substrates. IEEE Photon J 5(2):2600111
4. Cao W, Biser JM, Ee YK, Li X-H, Tansu N, Chan HM et al (2011) Dislocation structure of GaN films grown on planar and nano-patterned sapphire. J Appl Phys 110(5):053505
5. Lu T, Li S, Liu C, Zhang K, Xu Y, Tong J et al (2012) Advantages of GaN based light-emitting diodes with a p-InGaN hole reservoir layer. Appl Phys Lett 100(14):141106
6. Jiang Y, Li Y, Li Y, Deng Z, Lu T, Ma Z et al (2015) Realization of high-luminous-efficiency InGaN light-emitting diodes in the "green gap" range. Sci Rep 5:10883
7. Jin Y, Li Q, Li G, Chen M, Liu J, Zou Y et al (2014) Enhanced optical output power of blue light-emitting diodes with quasi-aligned gold nanoparticles. Nanoscale Res Lett 9(1):7
8. Zhao Y, Yun F, Wang S, Feng L, Su X, Li Y et al (2016) Mechanism of hole injection enhancement in light-emitting diodes by inserting multiple hole-reservoir layers in electron blocking layer. J Appl Phys 119(10):105703
9. Zhao H, Liu G, Tansu N (2010) Analysis of InGaN-delta-InN quantum wells for light-emitting diodes. Appl Phys Lett 97(13):131114
10. Zhao H, Tansu N (2010) Optical gain characteristics of staggered InGaN quantum wells lasers. J Appl Phys 107(11):113110
11. Rossow U, Hoffmann L, Bremers H, Buß ER, Ketzer F, Langer T et al (2015) Indium incorporation processes investigated by pulsed and continuous growth of ultrathin InGaN quantum wells. J Cryst Growth 414(4):49–55
12. Du C, Ma Z, Zhou J, Lu T, Jiang Y, Zuo P et al (2014) Enhancing the quantum efficiency of InGaN yellow-green light-emitting diodes by growth interruption. Appl Phys Lett 105(7):071108
13. Ting SM, Ramer JC, Florescu DI, Merai VN, Albert BE, Parekh A et al (2003) Morphological evolution of InGaN/GaN quantum-well heterostructures grown by metalorganic chemical vapor deposition. J Appl Phys 94(3):1461–1467
14. Kumar MS, Lee YS, Park JY, Chung SJ, Hong C-H, Suh E-K (2009) Surface morphological studies of green InGaN/GaN multi-quantum wells grown by using MOCVD. Mater Chem Phys 113(1):192–195
15. Cho HK, Lee JY, Kim CS, Yang GM (2002) Influence of strain relaxation on structural and optical characteristics of InGaN/GaN multiple quantum wells with high indium composition. J Appl Phys 91(3):1166–1170
16. Li X, Zhao DG, Yang J, Jiang DS, Liu ZS, Chen P et al (2016) Influence of InGaN growth rate on the localization states and optical properties of InGaN/GaN multiple quantum wells. Superlattices Microstruct 97:186–192
17. Lin Y, Zhou S, Wang W, Yang W, Qian H, Wang H et al (2015) Performance improvement of GaN-based light-emitting diodes grown on Si (111) substrates by controlling the reactor pressure for the GaN nucleation layer growth. J Mater Chem C 3(7):1484–1490
18. Lu T, Ma Z, Du C, Fang Y, Wu H, Jiang Y et al (2014) Temperature-dependent photoluminescence in light-emitting diodes. Sci Rep 4:6131
19. Lin T, Kuo HC, Jiang XD, Jiang XD, Feng ZC (2017) Recombination pathways in green InGaN/GaN multiple quantum wells. Nanoscale Res Lett 12(1):137
20. Scholz F, Off J, Fehrenbacher E, Gfrörer O, Brockt G (2000) Investigations on structural properties of GaInN-GaN multi quantum well structures. Phys Stat Sol (a) 180(1):315–320
21. Suihkonen S, Lang T, Svensk O, Sormunen J, Törmä PT, Sopanen M et al (2007) Control of the morphology of InGaN/GaN quantum wells grown by metalorganic chemical vapor deposition. J Cryst Growth 300(2):324–329
22. Daele BV, Tendeloo GV, Jacobs K, Moerman I, Leys MR (2004) Formation of metallic In in InGaN/GaN multiquantum wells. Appl Phys Lett 85(19): 4379–4381
23. Kumar MS, Park JY, Lee YS, Chung SJ, Hong C-H, Suh E-K (2007) Effect of barrier growth temperature on morphological evolution of green InGaN/GaN multi-quantum well heterostructures. J Phys D Appl Phys 40(17):5050–5054
24. Czernecki R, Grzanka E, Smalc-Koziorowska J, Grzanka S, Schiavon D, Targowski G et al (2015) Effect of hydrogen during growth of quantum barriers on the properties of InGaN quantum wells. J Cryst Growth 414:38–41
25. Lv W, Wang L, Wang J, Hao Z, Luo Y (2012) InGaN/GaN multilayer quantum dots yellow-green light-emitting diode with optimized GaN barriers. Nanoscale Res Lett 7(1):617
26. Ren P, Zhang N, Xue B, Liu Z, Wang J, Li J (2016) A novel usage of hydrogen treatment to improve the indium incorporation and internal quantum efficiency of green InGaN/GaN multiple quantum wells simultaneously. J Phys D Appl Phys 49(17):175101
27. Suihkonen S, Svensk O, Lang T, Lipsanen H, Odnoblyudov MA, Bougrov VE (2007) The effect of InGaN/GaN MQW hydrogen treatment and threading dislocation optimization on GaN LED efficiency. J Cryst Growth 298(1):740–743
28. Czernecki R, Kret S, Kempisty P, Grzanka E, Plesiewicz J, Targowski G et al (2014) Influence of hydrogen and TMIn on indium incorporation in MOVPE growth of InGaN layers. J Cryst Growth 402(402):330–336
29. Hu Y-L, Farrell RM, Neufeld CJ, Iza M, Cruz SC, Pfaff N et al (2012) Effect of quantum well cap layer thickness on the microstructure and performance of InGaN/GaN solar cells. Appl Phys Lett 100(16):161101
30. Pan Z, Wang YT, Zhuang Y, Lin YW, Zhou ZQ, Li LH et al (1999) Investigation of periodicity fluctuations in strained $(GaNAs)_1(GaAs)_m$ superlattices by the kinematical simulation of x-ray diffraction. Appl Phys Lett 75(2):223–225
31. Lin F, Xiang N, Chen P, Chow SY, Chua SJ (2008) Investigation of the V-pit related morphological and optical properties of InGaN/GaN multiple quantum wells. J Appl Phys 103(4):043508
32. Chen Y, Takeuchi T, Amano H, Akasaki I, Yamada N, Kaneko Y et al (1998) Pit formation in GaInN quantum wells. Appl Phys Lett 72(6):710–712
33. Liliental-Weber Z, Chen Y, Ruvimov S, Washburn J (1997) Formation mechanism of nanotubes in GaN. Phys Rev Lett 79(15):2835–2838
34. Sun CJ, Zubair Anwar M, Chen Q, Yang JW, Asif Khan M, Shur MS et al (1997) Quantum shift of band-edge stimulated emission in InGaN–GaN multiple quantum well light-emitting diodes. Appl Phys Lett 70(22):2978–2980
35. Wu XH, Elsass CR, Abare A, Mack M, Keller S, Petroff PM et al (1998) Structural origin of V-defects and correlation with localized excitonic centers in InGaN/GaN multiple quantum wells. Appl Phys Lett 72(6):692–694
36. Morishita Y, Nomura Y, Goto S, Katayama Y (1995) Effect of hydrogen on the surface-diffusion length of Ga adatoms during molecular-beam epitaxy. Appl Phys Lett 67(17):2500–2502
37. Shiojiri M, Chuo CC, Hsu JT, Yang JR, Saijo H (2006) Structure and formation mechanism of V defects in multiple InGaN / GaN quantumwell layers. J Appl Phys 99(7):073505
38. Wang HX, Amijima Y, Ishihama Y, Sakai S (2001) Influence of carrier gas on the morphology and structure of GaN layers grown on sapphire substrate by six-wafer metal organic chemical vapor deposition system. J Cryst Growth 233(7):681–686
39. Koukitu A, Taki T, Takahashi N, Seki H (1999) Thermodynamic study on the role of hydrogen during the MOVPE growth of group III nitrides. J Cryst Growth 197(1):99–105
40. Sangwal K (1987) Etching of crystals: theory, experiment and application
41. Yu C-C, Chu C-F, Tsai J-Y, Huang HW, Hsueh T-H, Lin C-F et al (2002) Gallium nitride nanorods fabricated by inductively coupled plasma reactive ion etching. Jpn J Appl Phys 41(41):L910–L912
42. Yeh Y-H, Chen K-M, Wu Y-H, Hsu Y-C, Yu T-Y, Lee W-I (2011) Hydrogen etching of GaN and its application to produce free-standing GaN thick films. J Cryst Growth 333(1):16–19
43. Yeh Y-H, Chen K-M, Wu Y-H, Hsu Y-C, Lee W-I (2011) Hydrogen etching on the surface of GaN for producing patterned structures. J Cryst Growth 314(1):9–12
44. Hiramatsu K, Nishiyama K, Motogaito A, Miyake H, Iyechika Y, Maeda T (1999) Recent developments in selective area growth and epitaxial lateral overgrowth of III-nitrides. Phys Stat Sol (a) 176(1):535–543
45. Tiginyanu I, Stevens-Kalceff MA, Sarua A, Braniste T, Monaico E, Popa V et al (2016) Self-organized three-dimensional nanostructured architectures in bulk GaN generated by spatial modulation of doping. ECS J Solid St Sci Technol 5(5):218–227
46. Bai J, Wang T, Sakai S (2000) Influence of the quantum-well thickness on the radiative recombination of InGaN/GaN quantum well structures. J Appl Phys 88(8):4729–4733
47. Meneghini M, Trivellin N, Pavesi M, Manfredi M, Zehnder U, Hahn B et al (2009) Leakage current and reverse-bias luminescence in InGaN-based light-emitting diodes. Appl Phys Lett 95(17):173507

48. Shapiro NA, Feick H, Hong W, Cich M, Armitage R, Weber ER et al (2003) Luminescence energy and carrier lifetime in InGaN/GaN quantum wells as a function of applied biaxial strain. J Appl Phys 94(7):4520–4529
49. Tawfik WZ, Song J, Lee JJ, Ha JS, Ryu S-W, Choi HS et al (2013) Effect of external tensile stress on blue InGaN/GaN multi-quantum-well light-emitting diode. Appl Surf Sci 283(14):727–731
50. Moon Y-T, Kim D-J, Song K-M, Kim D-W, Yi M-S, Noh D-Y et al (2000) Effect of growth interruption and the introduction of H_2 on the growth of InGaN/GaN multiple quantum wells. J Vac Sci Technol B 18(6):2631–2634
51. Piner EL, Behbehani MK, El-masry NA, Roberts JC, McIntosh FG, Bedair SM (1997) Impurity dependence on hydrogen and ammonia flow rates in InGaN bulk films. Appl Phys Lett 71(14):2023–2025

Submit your manuscript to a SpringerOpen journal and benefit from:

- ► Convenient online submission
- ► Rigorous peer review
- ► Immediate publication on acceptance
- ► Open access: articles freely available online
- ► High visibility within the field
- ► Retaining the copyright to your article

Submit your next manuscript at ► springeropen.com